

Detection of superhumps in XTE J1118+480 approaching quiescence

C. Zurita^{1*}, J. Casares¹, T. Shahbaz¹, R.M. Wagner³, C.B. Foltz⁴, P. Rodríguez-Gil¹, R.I. Hynes², P.A. Charles², E. Ryan⁵, G. Schwarz⁵, S.G. Starrfield⁶

¹*Instituto de Astrofísica de Canarias E-38200 La Laguna, Tenerife, Spain*

²*Department of Physics & Astronomy, University of Southampton, Southampton, UK*

³*Large Binocular Telescope Observatory, University of Arizona, Tucson, Arizona, USA*

⁴*MMT Observatory, University of Arizona, Tucson, Arizona, USA*

⁵*Steward Observatory, University of Arizona, Tucson, Arizona, USA.* ⁶*Department of Physics & Astronomy, Arizona State University, Tempe, Arizona*

24 October 2018

ABSTRACT

We present the results of our monitoring of the halo black-hole soft X-ray transient (SXT) XTE J1118+480 during its decline to quiescence. The system has decayed 0.5 mags from December 2000 to its present near quiescent level at $R \simeq 18.65$ (June 2001). The ellipsoidal lightcurve is distorted by an additional modulation that we interpret as a superhump of $P_{\text{sh}} = 0.17049(1)$ d i.e. 0.3% longer than the orbital period. This implies a disc precession period $P_{\text{prec}} \sim 52$ d. After correcting the average phase-folded light curve for veiling, the amplitude difference between the minima suggests that the binary inclination angle lies in the range $i = 71 - 82^\circ$. However, we urge caution in the interpretation of these values because of residual systematic contamination of the ellipsoidal lightcurve by the complex form of the superhump modulation. The orbital-mean $H\alpha$ profiles exhibit clear velocity variations with ~ 500 km/s amplitude. We interpret this as the first spectroscopic evidence of an eccentric precessing disc.

Key words: stars: accretion, accretion discs – binaries: close – stars: individual (XTE J1118+480) – X-rays: stars

1 INTRODUCTION

XTE J1118+480 is an important SXT for a number of reasons. It is at high galactic latitude ($b = 62.3^\circ$) which makes it the first halo black-hole binary, since it must be at $\simeq 1$ kpc above the galactic plane (Wagner et al. 2001; Mirabel et al. 2001). The low interstellar absorption allows for detailed multi-wavelength studies during outburst. The energy distribution from IR to UV is consistent with a combination of an optically thick disc plus synchrotron emission, whereas the EUV to X-ray spectrum is reminiscent of the low (hard) state of SXTs (Hynes et al. 2000). Since $L_x/L_{\text{opt}} \simeq 5$ compared to typically 500 for galactic low mass X-ray binaries (LMXBs), it has been suggested that it may be an Accretion Disc Corona (ADC) source seen at high inclination (Garcia et al. 2000). However, the detection of X-ray, UV and optical QPOs at 0.08 Hz suggest that the inner disc is directly visible. The UV variability lags the X-rays by 1–2 s, consistent

with reprocessing in the accretion disc (Haswell et al. 2000). The optical rise to outburst preceded the X-ray rise by ~ 10 d which allowed the size of the advective corona to be constrained to $\sim 1.2 \times 10^4$ Schwarzschild radii (Wren et al. 2001). The radial velocity curve of the companion star and the large mass function ($6.1 \pm 0.3 M_\odot$) demonstrates that XTE J1118+480 contains a black hole (McClintock et al. 2001; Wagner et al. 2001). Finally, the rotational velocity of the companion star implies a mass ratio of $q = 0.037 \pm 0.007$ (Orosz 2001).

Optical superhumps were observed during the outburst, changing shape and period (Uemura et al. 2000a). Superhumps are optical modulations first discovered in Dwarf Novae superoutbursts with a period a few percent longer than the orbital period and a non-sinusoidal shape. Since then, this phenomenon has been seen in decaying novae, AM CVn systems and novalike variables. Both the amplitude and shape of the superhump modulation change while the outburst declines. The most promising models in ex-

* e-mail: czurita@ll.iac.es

plaining the superhump behaviour assume that the accretion disc expands, due to the action of viscosity, to the 3:1 resonance radius and the eccentric disc is then forced to precess by perturbations from the secondary (e.g. Whitehurst & King, 1991). Superhump lightcurves can be explained by changes in the disc luminosity associated with the periodic deformation of the disc shape (e.g. Simpson & Wood, 1998). Since the resonance is only possible for small mass ratios, superhumps should also appear in SXTs, as has been confirmed by O’Donoghue & Charles (1996). Furthermore the strongest resonance (2:1) requires very extreme mass ratios ($q \leq 0.025$) which might be reached in some SXTs such as J1118+480 as we will discuss here.

In this paper we present the detection of superhumps in XTE J1118+480 when the system was approaching the quiescent state. This discovery provides the first solid evidence of a precessing disc in a SXT near quiescence. Superhumps in dwarf novae were traditionally thought never to be present in quiescence but recent observations (Patterson et al. 1995) have shown that superhumps can indeed persist into quiescence after a superoutburst has ended. The case of XTE J1118+480 may be analogous behaviour in the SXTs. A preliminary analysis of these data was reported in Casares et al. (2001).

2 OBSERVATIONS AND DATA REDUCTION

2.1 Photometry

J1118+480 was observed for a total of 53 nights in the period December 2000–June 2001, during the time when the system was approaching quiescence, mainly in the R -band with six different telescopes:

- the 0.82 m (IAC80) and the 1 m Optical Ground Station (OGS) telescopes, equipped with identical Thomson CCD cameras and using exposure times ranging from 300 to 1200 s, at Observatorio del Teide (Tenerife). The IAC80 and OGS were operated simultaneously for two whole nights in order to obtain $R-I$ colour information.

- the 2.5 m Nordic Optical Telescope (NOT) and the 1 m Jacobus Kapteyn Telescope (JKT) at Observatorio del Roque de los Muchachos (La Palma). The data at the NOT, which have the best time resolution, were taken with ALFOSC with exposure times of 30 and 60 s. At the JKT we used exposure times ranging from 90 to 600 s with the SITE2 detector.

- the 1.3 m McGraw-Hill Telescope (MGHT) at the MDM[†] Observatory (Arizona) and the 1.55 m Kuiper Telescope of the University of Arizona on Mount Lemmon. Photometry in the I band was obtained with the Kuiper using the 2k×2k CCD camera (2kBigCCD) and in R band with the McGraw-Hill Telescope and 2k×2k *Echelle* CCD camera. The exposure time for both sets was 300 s and the seeing was typically 0.8–1.5 arcsec.

In all cases we used 2×2 pixel binning to improve the

readout time. In Table 1 we present a log of the observations.

In total, the target was observed for over 70 orbital cycles. The individual images were de-biased and flat-fielded in the standard way, with the data reduction being performed within IRAF[‡]. The instrumental magnitudes were obtained using PSF photometry with the IRAF routine DAOPHOT (Stetson 1987) or optimal photometry (Naylor 1998) using the *Starlink* PHOTOM package. Differential light curves were constructed relative to a nearby comparison star. Light curves of this comparison star with respect to others were also obtained in order to check for variability from which we estimate that our differential photometry is accurate to ~ 1 per cent in all observations.

2.2 Spectroscopy

We observed J1118+480 using the blue channel CCD spectrograph on the 6.5 m Multiple Mirror Telescope[§] (MMT) at Arizona, on the nights of 2000 Nov 20, 30 and 2001 Jan 4. The seeing was typically 1 arcsec and a 1 arcsec wide slit was employed. Each 1440 s exposure was bracketed by a HeNeAr lamp spectrum which led to a wavelength calibration accurate to $5\text{--}7 \text{ km s}^{-1}$ rms. Spectra were also obtained on 2001 Jan 12, with the ISIS red channel of the 4.2 m William Herschel Telescope (WHT) at Observatorio del Roque de los Muchachos (La Palma). The slit width was 1.5 arcsec and wavelength calibration was checked with respect to night-sky emission lines to be within 10 km s^{-1} . Further details of these observations can be found in Wagner et al. 2001; A further 29 spectra were taken on 15 and 16 Apr 2001 with the Steward Observatory 2.3 m Bok Telescope on Kitt Peak equipped with the B&C Spectrograph. A 400 line mm^{-1} grating and 1.5 arcsec wide entrance slit were employed which yielded spectra covering the spectral region 4100–7400 Å at a spectral resolution of 5.5 Å. The exposure time was 1400 s in typically 1.4 arcsec seeing and photometric conditions. The spectroscopic dataset was completed with 49 spectra obtained on 27 and 28 Apr 2001 on the 4.2 m WHT using the ISIS red arm. A narrow slit (0.8 arcsec) aligned with the parallactic angle and with no comparison star in the slit, was used in combination with a 1200 line mm^{-1} grating. The wavelength calibration derived from arc lamps was checked against night sky lines and was accurate to 1 km s^{-1} (see table 2).

Standard IRAF procedures were used to de-bias the images and to remove the small scale CCD sensitivity variations. One dimensional spectra were extracted using the optimal extraction method (Horne 1986). Where possible we performed flux calibration relative to other stars on the slit.

[‡] IRAF is distributed by the National Optical Astronomy Observatories, which is operated by the Association of Universities for Research in Astronomy, Inc., under contract with the National Science Foundation.

[§] MMT is operated as a joint facility of the Smithsonian Institution and the University of Arizona by the Multiple Mirror Telescope Observatory.

[†] The MDM observatory is a joint facility of Dartmouth College, The University of Michigan, Columbia University and the Ohio State University.

Table 1. Log of photometric observations

<i>Night</i>	<i>Telescope</i>	<i>Filter</i>	<i>Exposure time (s)</i>	<i>Coverage (cycles)</i>
2000 Dec 13	IAC80	R	600	0.97
2000 Dec 14	IAC80	R	600	1.01
2000 Dec 28	IAC80	R	600	1.22
2001 Jan 09	IAC80	R	600	0.50
2001 Jan 11	IAC80	R	600	0.97
2001 Jan 19	IAC80	R	600	0.80
2001 Jan 27	IAC80	R	600	0.93
2001 Jan 31	IAC80	R	600	1.89
2001 Feb 01	IAC80	R	600	1.76
2001 Feb 02	IAC80	R	1200	1.58
2001 Feb 03	IAC80	R	900	1.76
2001 Feb 04	IAC80	R	600	1.35
2001 Feb 24	IAC80	R	600	1.01
2001 Feb 27	IAC80	R	600	0.34
2001 Mar 07	IAC80	R	1200	1.16
2001 Mar 08	IAC80	R	600	1.01
2001 Mar 09	IAC80	R	600	0.97
2001 Mar 10	IAC80	R	600	1.08
2001 Mar 11	IAC80	R	600	1.76
2001 Mar 18	Kuiper	I	300	1.50
2001 Mar 19	Kuiper	I	300	1.69
2001 Mar 20	Kuiper	I	300	1.37
2001 Mar 21	Kuiper	I	300	1.69
2001 Mar 25	IAC80	R	600	1.87
2001 Mar 26	IAC80	R	600	1.64
2001 Mar 28	IAC80	R	600	1.91
2001 Apr 01	NOT	R	30	2.02
2001 Apr 02	NOT	R	60	1.34
2001 Apr 04	IAC80	R	600	1.01
2001 Apr 05	OGS	R	300	0.83
2001 Apr 06	OGS	R	300	1.68
2001 Apr 07	OGS	I	300	1.76
2001 Apr 08	OGS	R	300	2.23
2001 Apr 09	OGS, IAC80	R, I	420, 420	1.85, 1.75
2001 Apr 10	OGS, IAC80	R, I	420, 600	2.00, 1.60
2001 Apr 11	IAC80	R	600	1.83
2001 Apr 12	IAC80	R	600	1.60
2001 Apr 13	IAC80, MGHT	R, R	600, 300	1.90, 1.59
2001 Apr 14	MGHT	R	300	1.26
2001 Apr 15	MGHT	R	300	0.89
2001 Apr 16	MGHT	R	300	1.72
2001 Apr 17	MGHT	R	300	1.69
2001 Apr 20	JKT	R	90–120	0.50
2001 Apr 22	JKT	R	90	1.86
2001 Apr 23	JKT	R	600	0.27
2001 Apr 24	JKT	R	90–600	1.77
2001 Apr 25	JKT	R	90–180	1.21
2001 Apr 27	JKT	R	180	1.12
2001 Apr 28	JKT	R	300	1.70
2001 May 29	IAC80	R	600	0.88
2001 May 30	IAC80	R	1200	0.91
2001 Jun 12	OGS	R	600	0.64
2001 Jun 26	IAC80	R	600	0.25

Absolute photometric calibration was not attempted due to slit losses.

3 PERIOD ANALYSIS

In Figure 1 we present the overall *R*-band lightcurve (nightly means) which shows that the system has been

steadily fading from its April 2000 outburst with a decay rate of $0.003 \text{ mag day}^{-1}$. After 25 Apr 2001 the rate of decay slowed and on 12 Jun 2001 the system was found at $R=18.650\pm 0.007$. The same magnitude was found, within the errors, on 26 Jun, so we suggest that this is the true quiescent magnitude. It is also consistent, within the errors, with the *R* magnitude from the USNO A2.0 catalogue, where

Table 2. Log of spectrometric observations

<i>Night</i>	<i>Telescope</i>	<i>Wavelength range (Å)</i>	<i>Resolution (Å/pix)</i>	<i>Exposure (s)</i>	<i>Number of spectra</i>
2000 Nov 20	MMT	λλ4200–7500	1.1	1440	5
2000 Nov 30	MMT	λλ4200–7500	1.1	1440	9
2001 Jan 04	MMT	λλ4200–7500	2.50	1440	6
2001 Jan 12	WHT	λλ5820–7320	1.47	1200	7
2001 Apr 15	Bok	λλ4100–7400	2.75	1400	14
2001 Apr 16	Bok	λλ4100–7400	2.75	1400	15
2001 Apr 27	WHT	λλ6300–6700	0.41	340–1000	23
2001 Apr 28	WHT	λλ6300–6700	0.41	340–1000	26

it is quoted as $R=18.8$ with about ~ 0.25 mag accuracy. Superimposed on the smooth decay, we also see substantial night to night variability.

Close inspection of the individual light curves shows the dominant ellipsoidal modulation of the companion star and a distortion wave which progressively moves across the orbital light curve. The distortion wave produces dramatic changes in the symmetry and minima in the light curves (see Fig. 4). As the distortion wave is most probably non-sinusoidal in nature we employed the PDM algorithm to separate and analyze the different periodicities present in the data.

We detrended the long-term variations by subtracting the nightly means from the individual lightcurves. This removed the low frequency peaks from our PDM spectrum in the top panel of Fig. 2 (computed in the frequency range 3 to 30 cycles d^{-1} with a resolution of 4×10^{-3} cycles d^{-1} and with 25 phase bins). The deepest minima are found at 5.885 cycles d^{-1} and 11.769 cycles d^{-1} which correspond to the orbital period (i.e. $P = 0.169936$ d) and the first harmonic respectively. A two-component Fourier series (with $P_2 = 2 \times P_1$; a first-order approximation to the ellipsoidal modulation of the secondary star) was fitted to the detrended lightcurve. The fit yielded $P_{\text{orb}} = P_1 = 0.169937(1)$ d and $T_0 = 2452022.5122(4)$, where T_0 corresponds to inferior conjunction of the companion star.

The bottom panel in Fig. 2 shows the PDM spectrum after subtracting these two Fourier components (P_{orb} and $P_{\text{orb}}/2$). A strong signal is found at $f = 5.865$ cycles d^{-1} and its harmonics. The fundamental frequency corresponds to 0.17049(1) d, 0.3% longer than the orbital period. Note that this period is comparable to periodicities reported during outburst (Uemura et al. 2000b) and hence we interpret it as the superhump period caused by a precessing eccentric disc. We note this is the first secure evidence of superhumps near quiescence in an SXT.

The light curve of the superhump was obtained through the following procedure: first we detrended the overall ellipsoidal lightcurve by subtracting the nightly mean magnitudes and then phase-folded it into 50 phase bins. This was fitted with a simple ellipsoidal model, fixing $i = 75^\circ$ and $q = 0.04$ (see top panel in Fig. 3). The ellipsoidal fit was subtracted from the overall (detrended) lightcurve and the residuals were then folded into 50 bins using the su-

perhump period of 0.17049d (bottom panel of Fig. 3). The lightcurve is clearly non-sinusoidal, and shows a peculiar modulation which explains why the PDM spectrum contained substantial power at the first and third harmonics. The shape is clearly different from the superhumps detected in other SXTs during outburst (e.g. O’Donoghue & Charles 1996). However, we note that our data were taken when J1118+480 was near true quiescence when such features are not usually visible. A clear evolution of the superhump from single humped modulation to a more complex shape had already been observed when the system started its decline[¶]. Peculiar superhump modulations, showing several peaks and dips are often detected in cataclysmic variables (CVs) and their origin remains unsolved (e.g. V603 Aql, Patterson et al. 1993; V503 Cygni, Harvey et al. 1995; H 0551-819, Patterson 1995).

Fig. 4 contains nightly lightcurves with superimposed model fits of a simple ellipsoidal lightcurve (dashed line) and a combination of ellipsoidal modulation plus superhump wave (continuous line). The superhump wave was simulated by a four term Fourier series fixing the superhump period at $P_{\text{sh}}=0.17049$ d. The second model is clearly a much more accurate representation of the observed lightcurves, with $\chi^2_{\nu}=1.71$ vs $\chi^2_{\nu}=3.08$. If the superhump modulation is due to tidal interactions in an elliptical precessing disc, and if the disc’s radius shrank as the system faded (as is shown in Fig. 1), we expect the shape and amplitude of the superhump modulation to change and even vanish if the disc radius decreases below the stability radius.

4 THE ELLIPSOIDAL MODULATION

The ellipsoidal light curve of the secondary star was phase folded and binned into 30 bins using our updated ephemeris (see section 3). It can be seen from Fig. 3 that the light curve of the superhump modulation is far from simple. It is clear that this will distort the ellipsoidal light curve, rendering it difficult to interpret since the superhump modulation could introduce false features in the light curve. This makes it very difficult to interpret any parameters derived from fitting the contaminated light curve. However, we can use the observed

[¶] see the lightcurves in <http://www.kusastro.kyoto-u.ac.jp/vsnet/Xray/xtej1118-camp.html>

amplitude of the modulation and an estimate for the veiling in order to place limits on the binary inclination.

The veiling for the photometric observations taken in April 2001 can be estimated by extrapolating the spectroscopic veiling observed in Jan 2001 (Wagner et al. 2001). J1118+480 decreased by 0.30 mags from Jan 2001 to April 2001. If we assume that this decrease in flux is solely due to the accretion disc light fading, then given the observed veiling in Jan 2001 of 67%, we estimate the veiling in April 2001 to be 53%. This value agrees very well with the veiling estimated from the high resolution WHT spectra taken in April 2001; $47 \pm 7\%$, obtained using the standard optimal subtraction technique (Marsh, Robinson & Wood 1994) for K5–M4 type template stars.

The large amplitude of the observed modulation strongly suggests that the inclination angle is high, but the lack of eclipse features at phase 0.0 requires $i \leq 82$ degrees (also note that no X-ray eclipses were seen during outburst). The difference between the two minima at phase 0.0 and phase 0.5 in the observed light curve is 0.076 mags. However, we have already noted that the observed light is heavily veiled ($47 \pm 7\%$) and so the true amplitude is in the range 0.127–0.165 mags. We have computed the secondary star’s ellipsoidal modulation assuming a K7v secondary star ($T_{\text{eff}}=4250$ K and $\log \bar{g}=5.0$; Wagner et al. 2001) and $q=0.037$ (Orosz 2001) using an irradiated X-ray binary model (for details see Shahbaz, 2002). By comparing the corrected amplitude with the calculated, we estimate an inclination angle in the range 71–84 degrees. Combined with the lack of eclipses this suggests that i lies in the range 71–82 degrees.

For more accurate results we would need to model the light curves free from the superhump modulation. However, deconvolving the two modulations is very difficult because in order to do so we have to be confident we have determined the ‘clean’ ellipsoidal light curve. This is only possible once we are sure that the system is completely in quiescence at which time we expect the amplitude of the superhump to be reduced.

5 $H\alpha$ VARIABILITY

Our spectra are dominated by strong double-peaked $H\alpha$ emission which exhibits significant time variability both in velocity and width. Some nights, for instance, the $H\alpha$ centroid and FWHM are modulated with the orbital period whereas other nights are consistent with a double sine-wave modulation. In addition, the FWHM and line centroid is seen to vary by a few hundred km s^{-1} from night to night. Although near quiescence, the accretion disc still contributes significantly to the observed optical emission and we see a 0.5 mag fading in the course of our campaign. This is well depicted by the equivalent width evolution of the $H\alpha$ emission line, which shows a continuous rise of $\sim 0.14 \text{ \AA day}^{-1}$ due to the continuum decay (Fig. 5). We also note that the $H\alpha$ line moves dramatically from night to night as is shown in Fig. 6 and Fig. 7. Here a three-component Gaussian fit to the nightly averaged profiles was performed, consisting of a broad base and two narrow peaks. The line is clearly asymmetric with the blue peak persistently stronger than the red one. We have computed the position of narrow peaks and

the line centroids given by our fits to the averaged profiles, to measure the real line velocity change and not the flux weighted centroids. The line centroids move from night to night with variations of ~ 500 km/s amplitude. If the nightly drifts of the emission lines are due to an eccentric disc projecting different amounts of its area at different precessing phases, we would expect the variation is modulated with a half of the precession period (~ 26 days). The line centroids are consistent with this period with minimum χ^2 (showing in Fig. 5, top panel), although we note that our spectroscopic sample is not sufficient to rule out a 52 d period (also shown in Fig. 5).

6 DISCUSSION

This paper presents evidence for an eccentric precessing disc in J1118+480 during Dec 2000 – June 2001. Although persistent superhumps have been detected in several extreme mass ratio CVs (i.e. Skillman & Patterson 1993) and there is some evidence for a superhump in the SXT A0620-00 during quiescence (Haswell 1996), this is, to our knowledge, the most extensive study of a precessing disc in SXTs near quiescence. Our lightcurve shows the fingerprint of a distorting superhump modulation with $P_{\text{sh}} = 0.17049(1)$ d superimposed on the classical ellipsoidal modulation of the secondary star. A superhump modulation with $P_{\text{sh}} = 0.17078(4)$ d was already detected in April 2000, when the system was at the peak of its outburst (Uemura et al. 2000b). This implies a superhump period change of $\dot{P} \simeq -10^{-6}$ which is slower but comparable to typical values in SU UMa stars (Warner 1985). Since the superhump is the beat frequency between the orbital and disc precession frequency, the disk precession period is, therefore given by $P_{\text{prec}} = (P_{\text{orb}}^{-1} - P_{\text{sh}}^{-1})^{-1} \approx 52$ d.

The superhump period contains information on the mass ratio q . We can use the relation of Mineshige, Hirose & Osaki 1992 (hereafter M92) to estimate the mass ratio:

$$\Delta P = \frac{P_{\text{sh}} - P_{\text{orb}}}{P_{\text{orb}}} \simeq \frac{q}{4\sqrt{1+q}} \eta^{3/2}, \quad (1)$$

where ΔP is the period excess and η is the disc radius in terms of the critical disc radius for the 3:1 resonance. If we take $P_{\text{sh}} = 0.17078(4)$ d (Uemura et al. 2000b) as the true superhump period at outburst peak and the empirical value $\eta \simeq 0.8$ (see M92), we find $q \simeq 0.028$. A similar result is obtained using Patterson’s (2001) relation, i.e.,

$$\Delta P^{-1} = \left[\frac{P_{\text{sh}} - P_{\text{orb}}}{P_{\text{orb}}} \right]^{-1} = \left[\frac{0.37 q}{(1+q)^{1/2}} \right]^{-1} \eta^{-2.3} - 1, \quad (2)$$

For q in the range 0.04–0.30 he finds

$$\Delta P = 0.216(\pm 0.018) q \quad (3)$$

for systems with accurate determinations for q (i.e. $\eta = 0.8$). Extrapolating the above expression to J1118+480 we find $q=0.023 \pm 0.002$. This implies the most extreme mass ratio in this class, although we note that for $q \leq 0.025$ the 2:1 resonance rather than the classical 3:1 resonance would be the dominant tidal instability (Whitehurst & King 1991).

The mass ratio has been determined spectroscopically by Orosz (2001) using the rotational broadening of the secondary stars photospheric absorption lines; $q = 0.037 \pm$

0.007. This is comparable to, but less extreme than, the mass ratio determined using the superhump period excess, but we note that the former is dominated by our assumption for η , thus refined calibrations at the highest and lowest ΔP , in eq. 2 are needed. In this sense J1118+480 is a key system in the study of superhumps, since it allows us to extrapolate the 3:1 resonance instability close to the limit where the 2:1 resonance should start to dominate. In Fig. 8 we show the ΔP - q values for SXTs (O'Donoghue & Charles 1996 and this paper) and CVs (Patterson 2001; Molnar & Koblunicky 1992 and references therein), including only those systems with reliable q determinations. J1118+480 seems to agree well with both theoretical ΔP - q curves for $\eta = 0.8$.

The nightly mean H_α profiles are shown to move by up to $\pm 250 \text{ km s}^{-1}$, an effect which has not been seen before in any SXT or CV. This behavior is probably driven by the changing asymmetric disc brightness distribution also seen in our trailed spectra. If the effect we are seeing is the spectroscopic signature of an eccentric disc in J1118+480 precessing on a period of 52 d, we would expect a modulation consistent with this period as we can see in Fig. 5. In addition, the FWHM of the H_α line changes by a few hundred km s^{-1} both with the orbital and precession phase. Since the FWHM gives a measurement of the velocity dispersion in the disc, the observed variability is probably related to changes in the disc's shape, since the eccentric disc presents differing aspects of its projected area to the observer on both the superhump and precession periods.

7 ACKNOWLEDGMENTS

We are grateful to the IAC support astronomers who undertake the Service Programme at Izaña for obtaining some of the lightcurves that were used in this analysis. We also thank R. Corradi for taking the WHT spectra on Jan 9 and Brian McLean for agreeing to swap JKT nights so that simultaneous WHT–JKT coverage was possible and for helping to obtain some of the JKT observations. The WHT and JKT are operated on the island of La Palma by the ING. NOT is operated on the island of La Palma jointly by Denmark, Finland, Iceland, Norway, and Sweden, in the Spanish Observatorio del Roque de los Muchachos of the Instituto de Astrofísica de Canarias. The IAC80 and OGS telescopes are operated on the island of Tenerife by the IAC in the Spanish Observatorio de Izaña. TS acknowledges support by a *Marie Curie* fellowship HP-MF-CT-199900297. RIH and PAC acknowledge support for grant F/00-180/A from the Leverhulme Trust. SGS also acknowledges support from NSF and NASA aparts to ASU.

REFERENCES

Casares J., Zurita C., Shahbaz T., Rodriguez–Gil P., Charles P., Hynes R.I., Wagner R.M., Ryan E., Foltz C., Starrfield S., 2001, IAUC, 7617
 Garcia, M., Brown, W., Pahre M., McClintock J., Callanan P., Garnavich P., 2000, IAUC 7392
 Harvey D, Skillman D.R., Patterson J., Ringwald F.A., 1995, PASP, 107, 551

Haswell C.A., King A.R., Murray J.R., Charles P.A., 2001, MNRAS, 321, 475
 Haswell C.A., Skillman D., Patterson J., Hynes R.I., Cui W., 2000, IAUC 7427
 Haswell C.A., 1996, IAU Symp. 165: Compact Stars in Binaries, 165, 351
 Horne K., 1986, PASP, 98, 609
 Hynes R.I., Mauche C.W., Haswell C.A., Shrader C.R., Cui W., Chaty S., 2000, ApJ, 539, L37
 Kuulkers, E. 2001 (astro-ph/0102066)
 Lucy L.B., 1966, Zeitschrift Astrophysics, 65, 89
 Marsh T.R., Horne K., 10988, MNRAS, 235, 269
 Marsh T.R., Robinson E.L., Wood, J.H., 1994, MNRAS, 266, 137
 McClintock J.E., Garcia M.R., Caldwell N., Falco E.E., Garnavich P.M., Zhao P., 2001, ApJ, 551, L147
 Mineshige S., Hirose M., Osaki Y., 1992, PASJ, 44, L15
 Mirabel I.F., Dhawan V., Mignani R.P., Rodrigues I., Guglielmetti F., 2001, Nature, 413, 139
 Molnar L.A., Koblunicky H.A., 1992, ApJ, 392, 678
 Naylor T., 1998, MNRAS, 296, 339
 Neustroev V.V., Borisov N.V., Barwig H., Bobinger A., Mantel K.H., Šimić D., Wolf S., 2001, astro-ph/0110111
 O'Donoghue D., Charles P.A., 1996, MNRAS, 282, 191
 Orosz J.A., 2001, ATEL 67
 Osaki Y., 1985, A&A, 144, 369
 Patterson J., 2001, PASP, 113, 736
 Patterson J., 1995, PASP, 107, 657
 Patterson J., Jablonski F., Koen C., O'Donoghue D., Skillman D.R., 1995, PASP, 107, 1183
 Patterson J., Thomas G., Skillman D.R., Diaz M.P., 1993, ApJS, 86, 235
 Shahbaz T. et al., 2002, in preparation
 Simpson J.C, Wood M.A., 1998, ApJ, 506, 360
 Skillman D.R., Patterson J., 1993, ApJ, 417, 298
 Stellingwerf R.F., 1978, ApJ, 224, 953
 Steeghs D., Harlaftis E.T., Horne K. 1997, MNRAS, 290, L28
 Stetson P.B., 1987, PASP, 99, 191
 Thorstensen J.R., Taylor C.J., 1997, PASP, 109, 1359
 Torres M.A.P et al., 2001, ApJ, submitted
 Uemura M., Kato T., Matsumoto K., Honkawa M., Cook L., Martin B., Masi G., Oksanen A., Moilanen M., Novak R., Sano Y., Ueda Y., 2000, IAUC 7418
 Uemura M., Kato T., Matsumoto K., Yamaoka H., Takamizawa K., Sano Y., Haseda K., Cook L.M., Buczynski D., Masi G., 2000 PASJ, 52, L15
 Wagner R.M., Foltz C.B., Shahbaz T., Casares J., Charles P.A., Starrfield S.G., Hewett P., 2001, ApJ, 556, 42
 Warner B., 1985, in Eggleton P.P., Pringle J.E., eds., *Interacting Binaries*. Reidel, Dordrecht, p. 367
 Whitehurst R., King A.R., 1991, MNRAS, 249, 25
 Wren J., Akerlof C., Balsano, R., Bloch J., Borozdin K., Casperson D., Gisler G., Kehoe R., Lee B.C., Marshall S., McKay T., Priedhorsky W., Rykoff E., Smith D., Trudolyubov S., Vestrand W.T., 2001, astro-ph/0105420

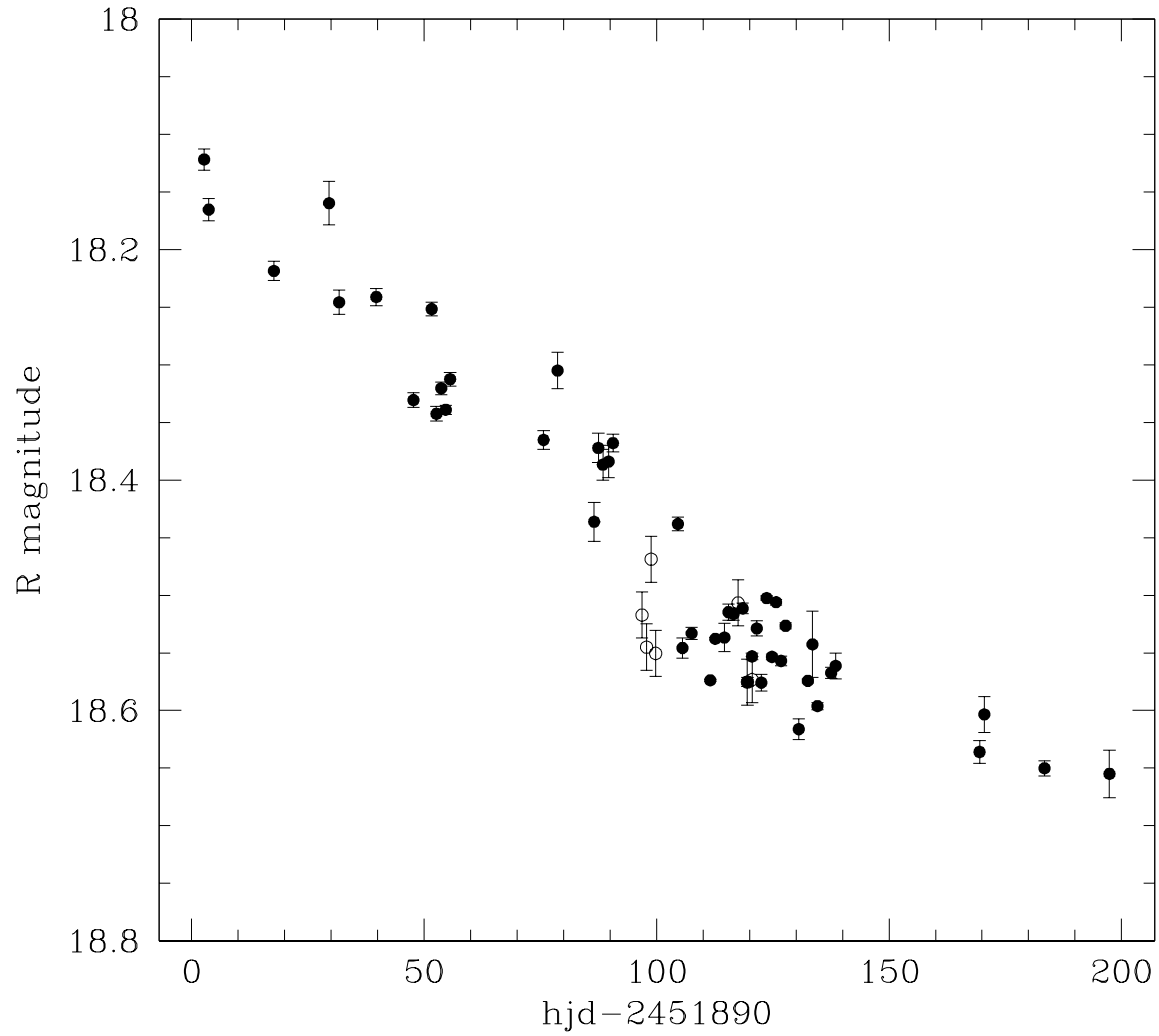


Figure 1. Long-term decay in the lightcurve of J1118+480 from Dec 2000 – June 2001. Only nightly means are shown. Open circles represent I-band observations, where a colour correction of $R-I=-0.24$ has been applied (based on our simultaneous R and I light curves of 9 and 10 April 2001).

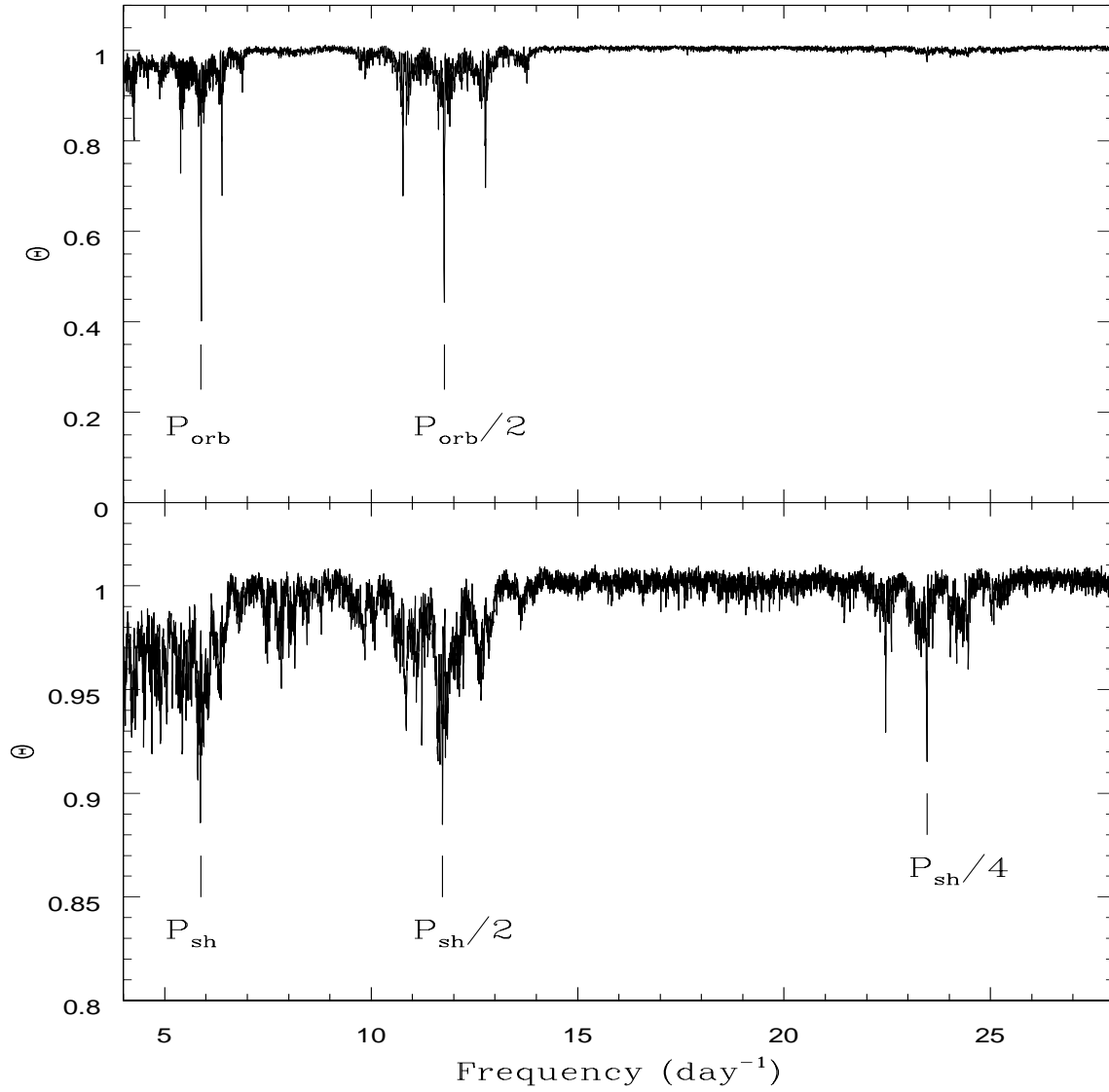


Figure 2. Top panel: PDM spectrum of the whole photometric data base after detrending long-term variations by subtraction of the nightly means. Bottom panel: Same but after subtracting the orbital and ellipsoidal ($P_{\text{orb}}/2$) frequencies. The deepest minima are marked, corresponding to the superhump frequency (P_{sh}) and its multiples $2f$ and $4f$.

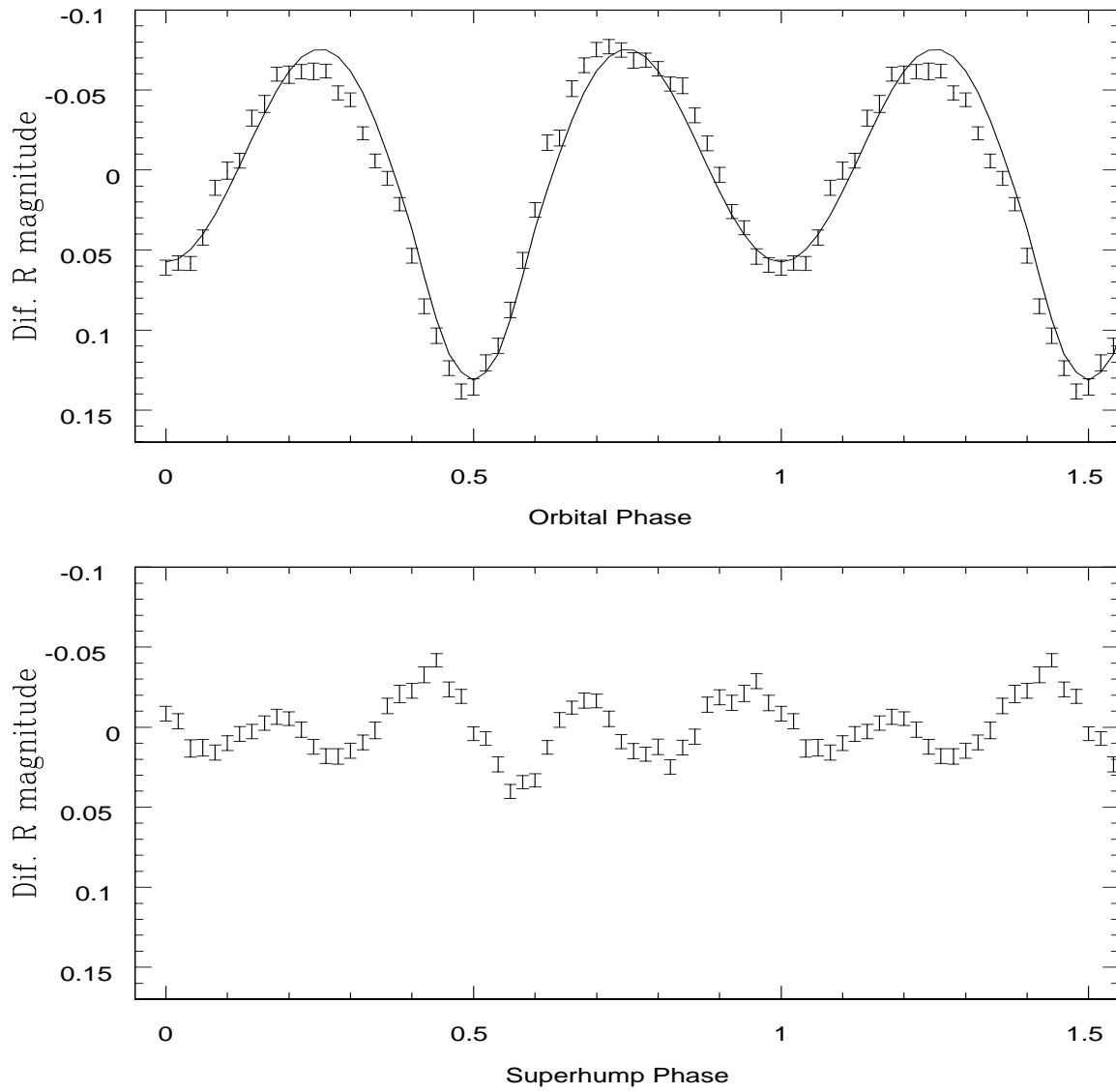


Figure 3. Top panel: Detrended lightcurve folded into 50 phase bins and fit with an ellipsoidal model (for $i = 75^\circ$ and $q = 0.04$). Bottom panel: Light curve of the superhump after subtracting the previous ellipsoidal model from the detrended light curve.

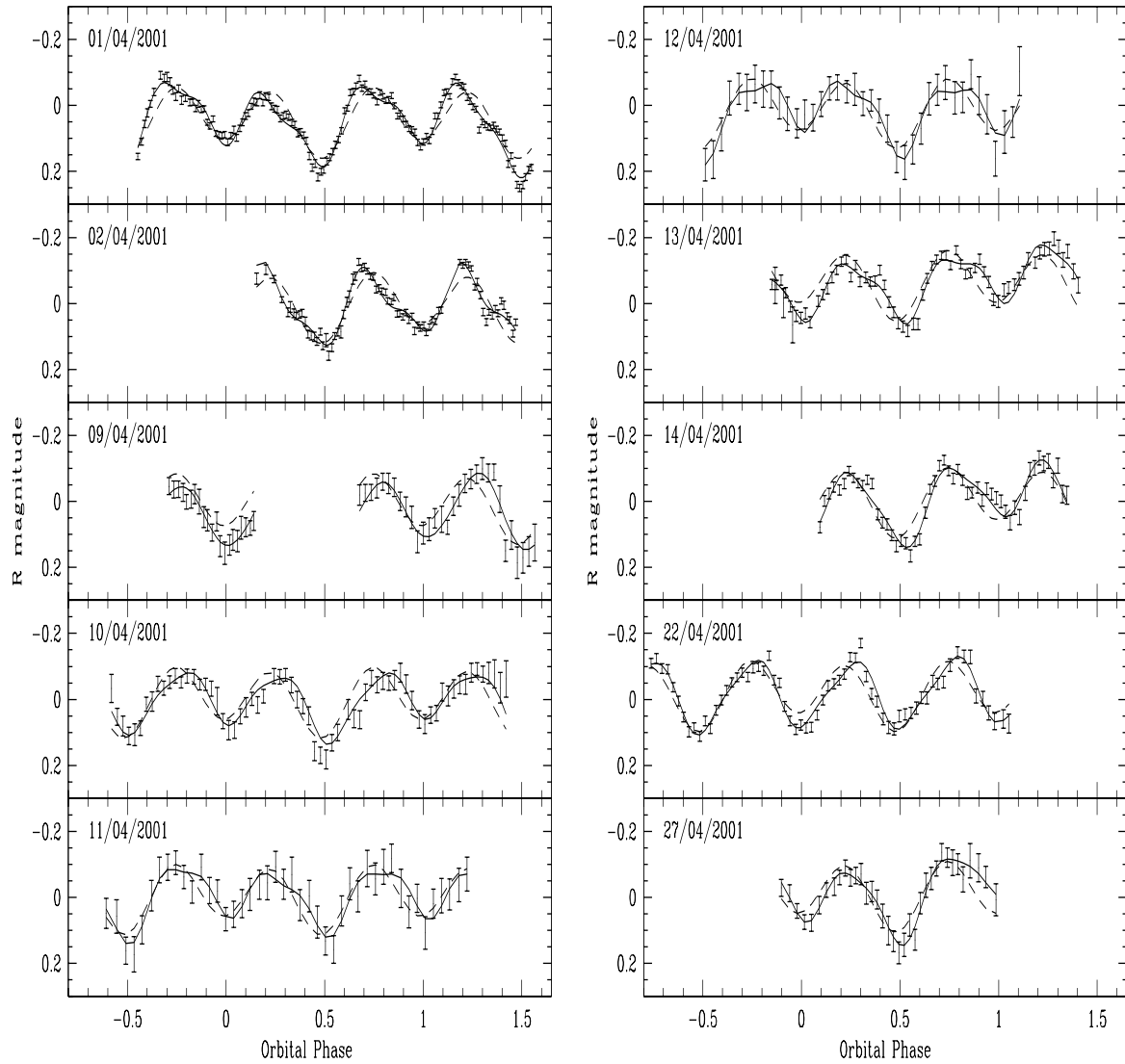


Figure 4. Orbital lightcurves for a sample of individual nights and best-fit models. Dashed line: ellipsoidal model. Continuous line: ellipsoidal model plus superhump wave.

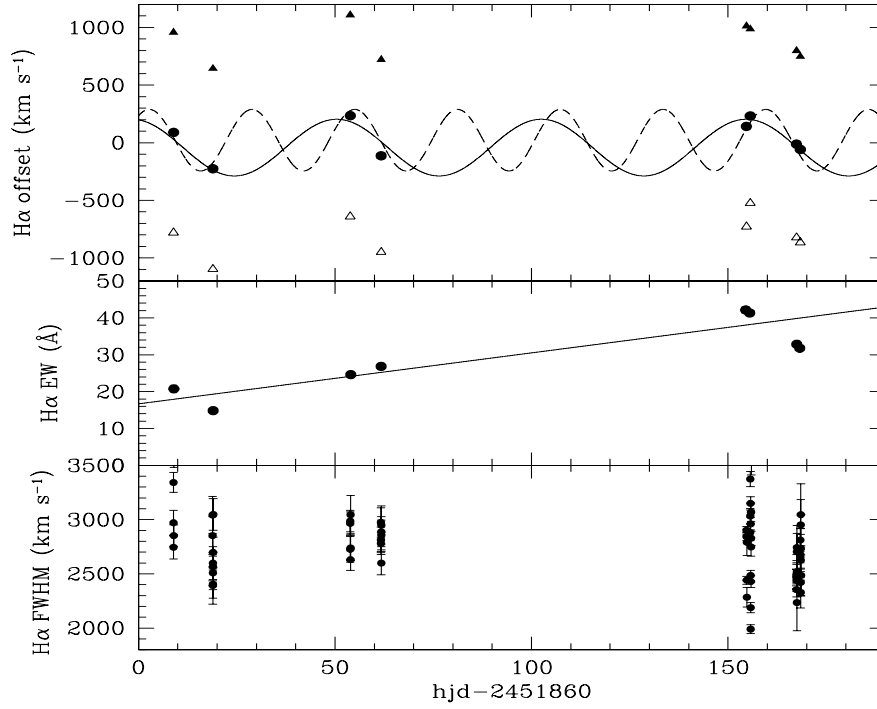


Figure 5. From top to bottom: $H\alpha$ centroids (filled circles) and double gaussians peaks (triangles) together with sinusoidal fits of $P=26$ days (dashed line) and $P=52$ days (solid line); mean equivalent width per night with the best linear fit and FWHM of individual spectra.

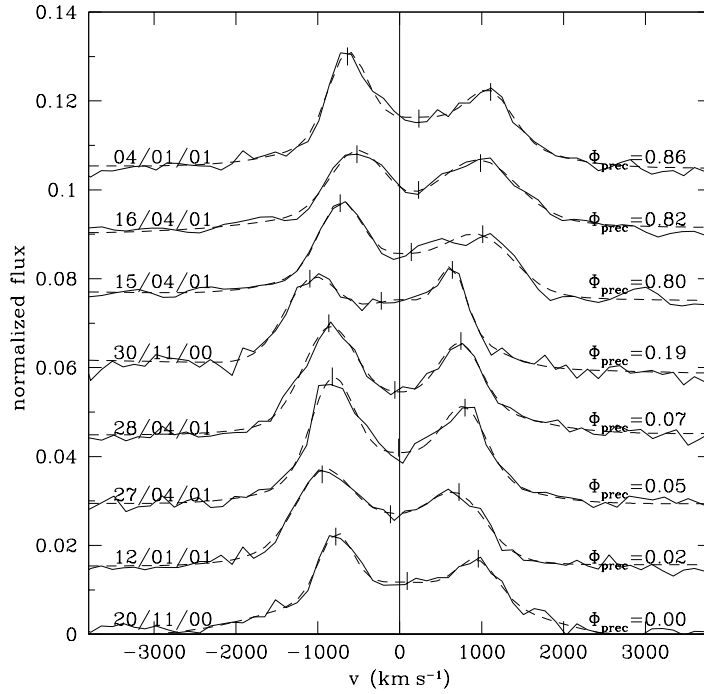


Figure 6. Averaged $H\alpha$ profiles and three-component fit for each night normalized by the equivalent width, where the positions of the peaks and the centroids have been marked. We have computed the phases for the precessing disc using a precession period of 52 d and an arbitrary phase 0.0.

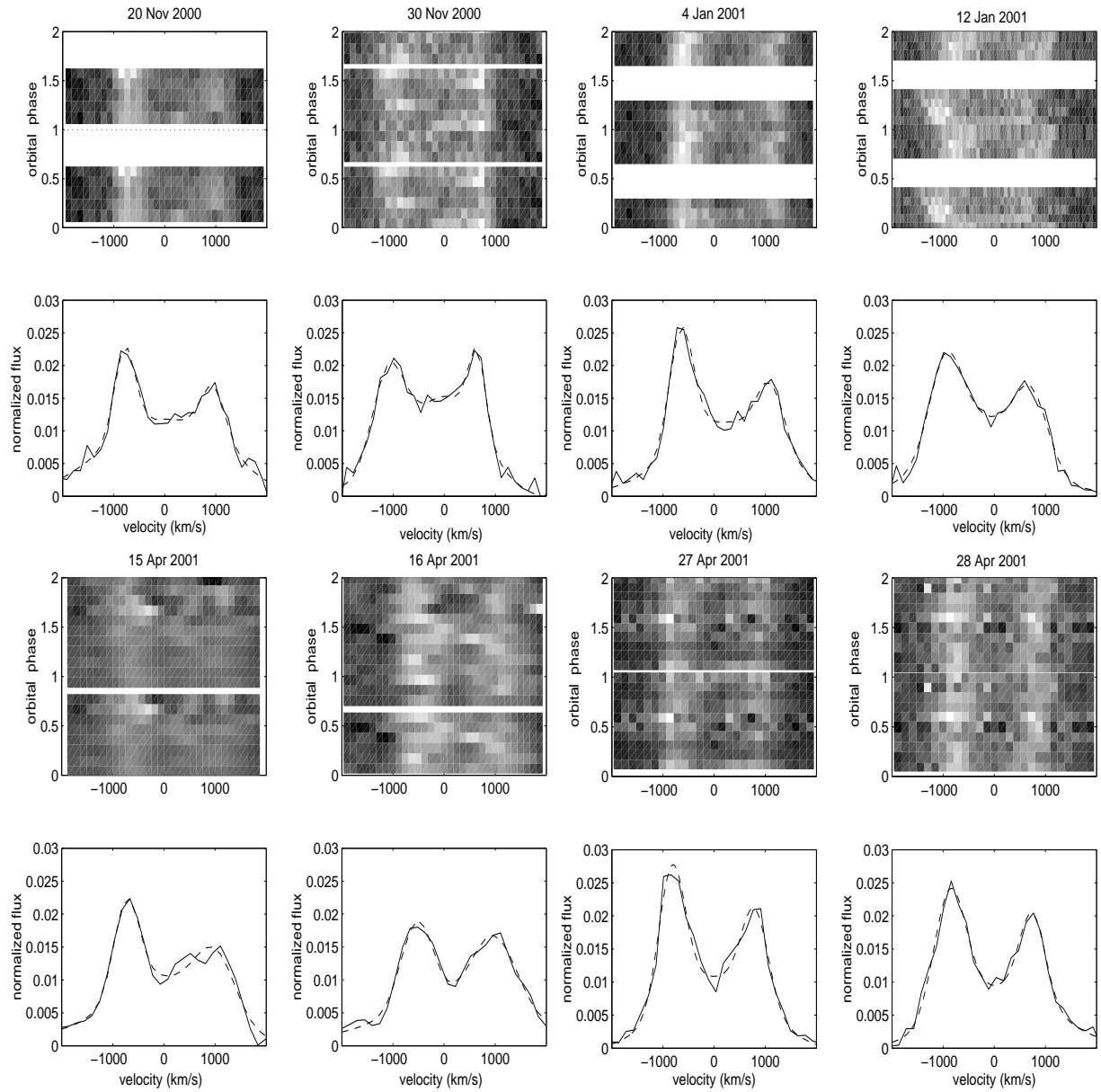


Figure 7. Upper panels: Observed trailed spectra. Lower panels: Averaged H α profiles and three-component fit for each night normalized by the equivalent width.

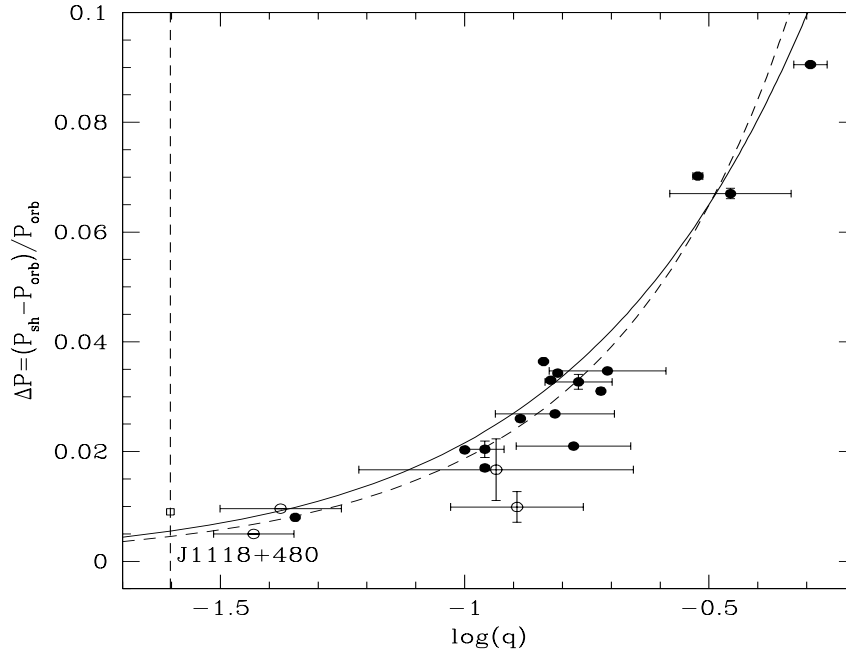


Figure 8. Relation between $\Delta P = (P_{sh} - P_{orb}) / P_{orb}$ and the mass ratio $q = M_2 / M_1$ for SU UMa stars (filled circles) and SXTs (open circles). The open square marks the dipping-bursting X-ray binary V1405 Aqr. The solid line shows the relation given by Patterson (2001) and the dashed line the relation by Osaki (1985) for $\eta = 0.8$. The vertical line marks the $q \leq 0.025$ limit for which the 2:1 resonance would be the dominant tidal instability. The systems plotted are: WZ Sge, OY Car, Z Cha, IY UMa, HT Cas, DV UMa, V2051 Oph, UU Aqr and V1405 Aqr (see Patterson 2001 and references therein); SW UMa, T Leo, V436 Cen, VW Hyi, WX Hyi and TU Men (see Molnar & Koblunicky 1991 and references therein) and VY Aqr (see Thorstensen & Taylor 1997)